



## Structure and breakup history of the rifted margin of West Antarctica in relation to Cretaceous separation from Zealandia and Bellingshausen plate motion

F. Wobbe and K. Gohl

*Alfred Wegener Institute for Polar and Marine Research, PO Box 120161, D-27515 Bremerhaven, Germany (fwobbe@awi.de)*

A. Chambord and R. Sutherland

*GNS Science, 1 Fairview Drive, Lower Hutt 5040, New Zealand*

[1] Geophysical data acquired using R/V Polarstern constrain the structure and age of the rifted oceanic margin of West Antarctica. West of the Antipodes Fracture Zone, the 145 km wide continent–ocean transition zone (COTZ) of the Marie Byrd Land sector resembles a typical magma-poor margin. New gravity and seismic reflection data indicates initial continental crust of thickness 24 km, that was stretched 90 km. Farther east, the Bellingshausen sector is broad and complex with abundant evidence for volcanism, the COTZ is ~670 km wide, and the nature of crust within the COTZ is uncertain. Margin extension is estimated to be 106–304 km in this sector. Seafloor magnetic anomalies adjacent to Marie Byrd Land near the Pahemo Fracture Zone indicate full-spreading rate during c33–c31 (80–68 Myr) of 60 mm yr<sup>-1</sup>, increasing to 74 mm yr<sup>-1</sup> at c27 (62 Myr), and then dropping to 22 mm yr<sup>-1</sup> by c22 (50 Myr). Spreading rates were lower to the west. Extrapolation towards the continental margin indicates initial oceanic crust formation at around c34y (84 Myr). Subsequent motion of the Bellingshausen plate relative to Antarctica (84–62 Myr) took place east of the Antipodes Fracture Zone at rates <40 mm yr<sup>-1</sup>, typically 5–20 mm yr<sup>-1</sup>. The high extension rate of 30–60 mm yr<sup>-1</sup> during initial margin formation is consistent with steep and symmetrical margin morphology, but subsequent motion of the Bellingshausen plate was slow and complex, and modified rift morphology through migrating deformation and volcanic centers to create a broad and complex COTZ.

**Components:** 11,300 words, 9 figures, 1 table.

**Keywords:** continent–ocean transition zone; crustal thickness; magnetic spreading anomaly; plate reconstruction.

**Index Terms:** 1517 Geomagnetism and Paleomagnetism: Magnetic anomalies: modeling and interpretation; 8105 Tectonophysics: Continental margins: divergent (1212, 8124); 8157 Tectonophysics: Plate motions: past (3040).

**Received** 6 June 2011; **Revised** 9 March 2012; **Accepted** 9 March 2012; **Published** 1 May 2012.

Wobbe, F., K. Gohl, A. Chambord, and R. Sutherland (2012), Structure and breakup history of the rifted margin of West Antarctica in relation to Cretaceous separation from Zealandia and Bellingshausen plate motion, *Geochem. Geophys. Geosyst.*, 13, Q04W12, doi:10.1029/2011GC003742.

**Theme:** Plate Reconstructions, Mantle Convection, and Tomography Models: A Complementary Vision of Earth's Interior

## 1. Introduction

[2] The formation of continental passive margins by rifting is affected by the rate of rifting, the initial configuration of continental lithosphere, and the temperature and composition of the asthenosphere [White *et al.*, 1992; van Wijk and Cloetingh, 2002]. The final breakup of Gondwana occurred during Late Cretaceous time as rifted continental crust of New Zealand separated from Antarctica at an intermediate-rate spreading ridge to produce typical oceanic crust [Molnar *et al.*, 1975; Cande *et al.*, 1995; Eagles *et al.*, 2004a; Sutherland *et al.*, 2010]. Hence, the region presents an ideal opportunity to study classical conjugate rifted margins, but this outcome has been frustrated by extreme logistic difficulties associated with collecting data adjacent to Antarctica. We present a substantial new marine geophysical dataset collected using R/V Polarstern, which has general relevance for the study of continental margins, has substantial regional implications, and adds to the body of knowledge required to construct reliable global plate kinematic estimates. Of particular regional interest is the complication of a small and short-lived oceanic plate, the Bellingshausen plate, which was active after break-up adjacent to the Antarctic margin.

[3] Geological samples, gravity data and receiver-function analysis of teleseismic earthquakes suggest that both West Antarctica [Llubes *et al.*, 2003; Luyendyk *et al.*, 2003; Winberry and Anandakrishnan, 2004; Block *et al.*, 2009] and the submarine plateaus surrounding New Zealand [Grobys *et al.*, 2009, and references therein] consist of extended continental crust. Widespread continental extension is thought to have been largely complete before the continental margins were formed and Zealandia drifted from Antarctica. Breakup reconstructions of Zealandia from Antarctica consider a narrow continent–ocean transition zone [Larter *et al.*, 2002; Eagles *et al.*, 2004a].

[4] In this study, we present new crustal thickness and density models of the Marie Byrd Land continental margin of Antarctica, and new magnetic anomaly interpretations from adjacent oceanic crust. The crustal thickness models provide a foundation for reconstructing the continent–ocean transition zone (COTZ), and hence better reconstructing the past positions of the conjugate continental fragments. Magnetic anomalies provide new constraints on the timing and rate of rifting during

continental margin formation, and on subsequent plate motions.

## 2. Data Acquisition and Processing

[5] During the Polarstern cruises in 2006 (ANT-23/4) and 2010 (ANT-26/3), ship- and airborne magnetic and shipborne gravity data have been acquired. These data were combined with seismic reflection and refraction/wide-angle reflection surveys from the same cruises to constrain the COTZ of Marie Byrd Land. Regions where measured ship-data are unavailable were filled with public domain satellite-derived free-air gravity data [Andersen and Knudsen, 2009], global seafloor topography data (version 13.1, 2010) [Smith and Sandwell, 1997], and ship-magnetic data from the GEODAS marine trackline geophysics database [National Geophysical Data Center, 2007]. Data acquisition and subsequent processing for each of the acquired datasets are described in the following sections.

### 2.1. Helicopter Magnetics

[6] In 2010, five thousand kilometers of aeromagnetic data were recorded at a sampling rate of 10 Hz during the North–South transit from New Zealand to the Amundsen Sea south of 69°S (Figures 1–5). A helicopter towed the optically pumped cesium vapor magnetometer 30 m below its airframe to avoid magnetic disturbances. Flight lines were arranged perpendicular to the expected magnetic lineation of the seafloor at an average line spacing of 10–20 km, covering a profile distance of about 450 km at a flight elevation of 100 m above sea level. Geographic position, speed and altitude of the aircraft as well as time were recorded at a rate of 5 Hz [Gohl, 2010].

[7] The cesium vapor magnetometer recorded data with a general heading error below 5 nT so that no calibration was necessary. Processing included removal of electromagnetic noise, resampling at 100 m intervals, and correction for the International Geomagnetic Reference Field using the IGRF-11 coefficients [Finlay *et al.*, 2010].

[8] Measured magnetic anomaly amplitudes of 50–400 nT were greater than the daily variation of 20–30 nT, observed at the Eyrewell Geomagnetic Observatory in New Zealand. Local daily variations were therefore considered negligible.

### 2.2. Shipborne Magnetics

[9] Two three-component fluxgate vector magnetometers mounted on the crow's nest of R/V

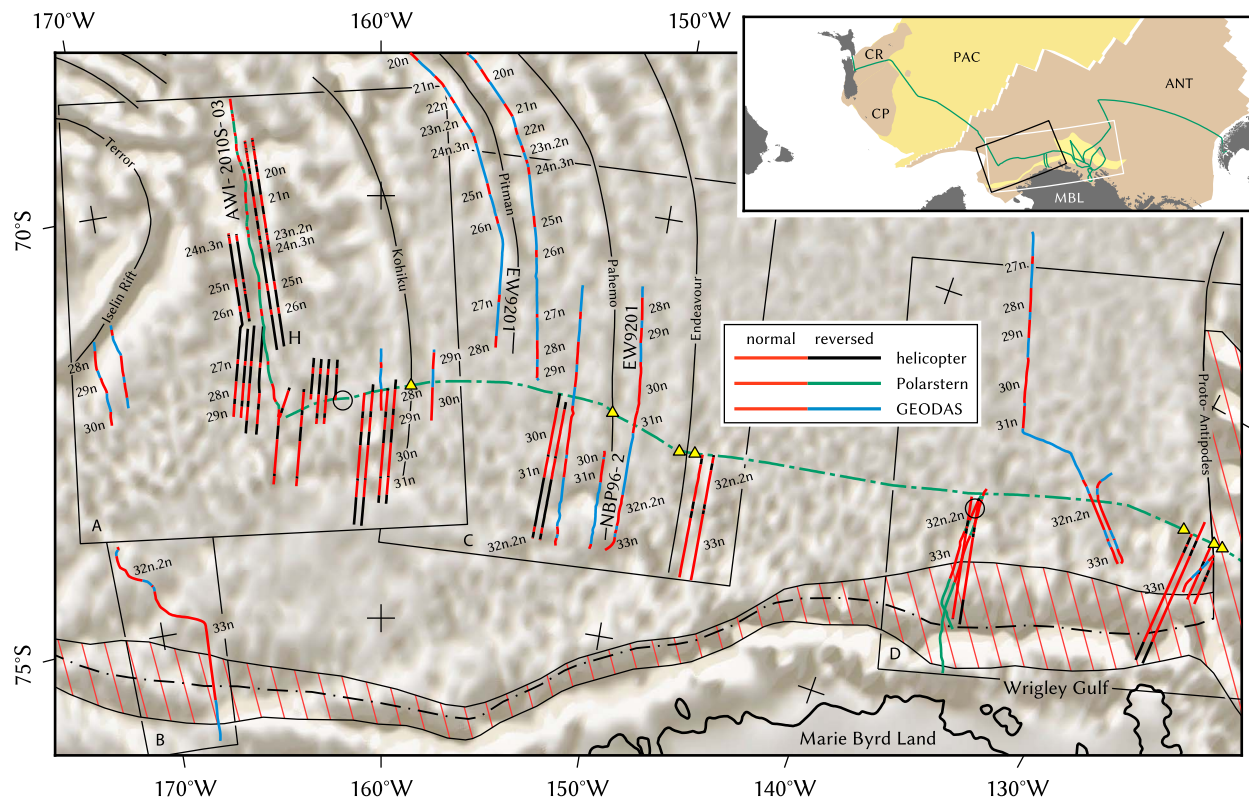


**Figure 1.** Identified magnetic spreading anomalies along helicopter- and ship-magnetic lines (R/V Polarstern lines AWI-2010S-00–AWI-2010S-03; GEODAS lines EW9201, NBP94-2, NBP96-2, NBP9702). Magnetic model of helicopter-magnetic line AWI-2010H-08-15-17 (H) and ship-magnetic line AWI-2010S-03 in Figure A.IX in Text S1 in the auxiliary material. Magnetic compensation loops during ANT-26/3 (circles); fracture zones (thin black lines); fracture zones evident in seismic lines AWI-20100110 and AWI-20100117 (yellow triangles); COTZ (striated area); and reconstructed pre-rift suture (dashed line). Black frames indicate locations of Figures 2–4. All features superimposed on DNSC08 satellite gravity map [Andersen and Knudsen, 2009]. Lambert conformal conic projection with central meridian 160°W and standard parallels 75°S and 69°S. Inset map shows ship track of R/V Polarstern expedition ANT-26/3 (green line); location of maps in Figure 1 and in Figure 6 (black and white frames); CP – Campbell Plateau; CR – Chatham Rise; ANT – West Antarctic plate; MBL – Marie Byrd Land; PAC – belonging to Pacific plate. Magnetic model of lines EW9201 and NBP96-2 in Figure A.VIII in Text S1 in the auxiliary material.

Polarstern measured shipborne magnetic data. The total magnetic field as well as the heading, roll, pitch, velocity, and position of the ship were logged at 1 Hz.

[10] Calibration loops provide coefficients relating the ship orientation (heading, roll, pitch) and speed to the variations in magnetometer measurements. To compensate for perturbations due to ship-induced magnetic fields, we measured a total of 13 calibration loops, five of which are located in our study area (Figure 6). During a calibration loop, the ship follows an eight-shaped course of two consecutive turns of opposite veer with a radius of about 1.8 km (1 NM) and a velocity of 5–7 kn.

[11] In the small area of a calibration loop, variations of the magnetic field due to crustal magnetization are considered negligible. In the larger area around the

calibration loop, the shipborne magnetic measurements were corrected with the motion coefficients according to König [2006]. The calibrated data have a maximum residual error of 20–30 nT under normal conditions at sea. Since the interference of the ship on the magnetic fields is larger than the daily magnetic variation, the daily variations were neglected in the determination of seafloor spreading anomalies.

[12] The induced magnetic field of the ship is not static, but instead depends on the strength, inclination, and declination of the ambient magnetic field. Since the inclination and declination show a high local variance in the higher latitudes, calibration coefficients are only adequate to fully correct their influence when the vessel operates inside a radius of 500–1500 km around the location of the calibration loop.

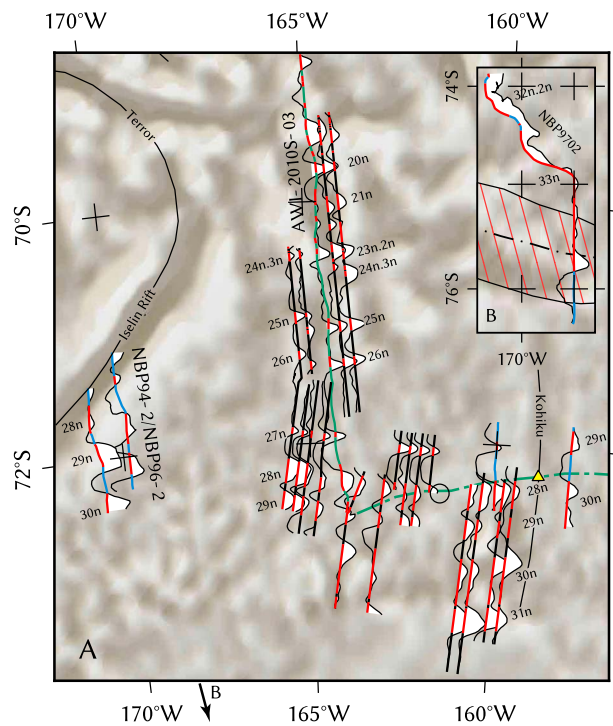


**Figure 2.** Magnifications of regions A and B in Figure 1. Magnetic identifications on top of measured anomalies along tracks; positive anomalies in white. Lambert conformal conic projection with central meridian 163°W and standard parallels 75°S and 69°S.

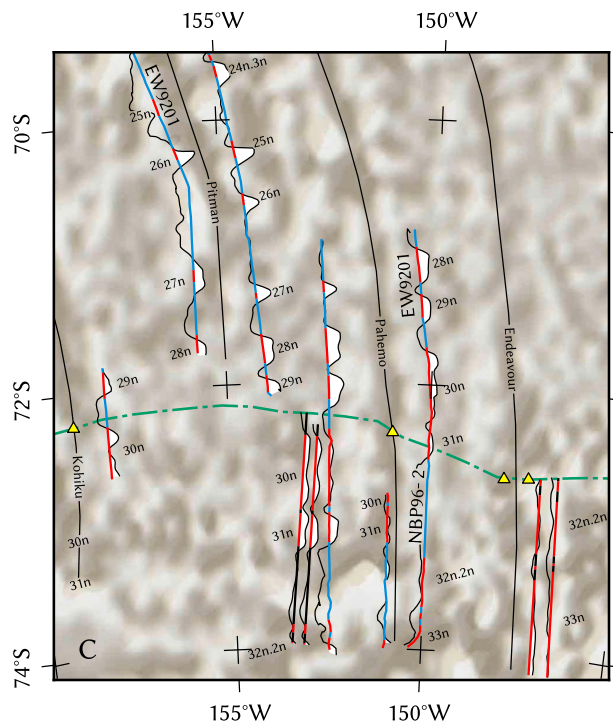


**Figure 3.** Magnification of region C in Figure 1. Lambert conformal conic projection with central meridian 152.5°W and standard parallels 75°S and 69°S.

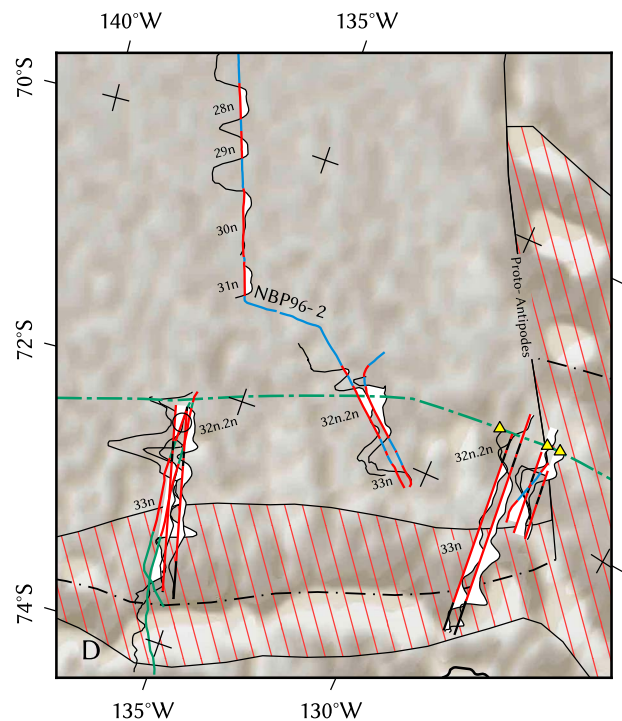


**Figure 4.** Magnification of region D in Figure 1. Lambert conformal conic projection with central meridian 155°W and standard parallels 75°S and 69°S.

[13] The necessity for carrying out a new calibration loop was determined by comparing the calibrated data from the two separate magnetometer sensors. Once the difference between both increased steadily, the set of calibration coefficients was insufficient to compensate the magnetic readings [Gohl, 2010].

[14] Some magnetic profiles retained long wavelength residual anomalies after processing, possibly due to the high regional variation in the geomagnetic field and the large operating area. The long wavelength anomalies were removed by leveling the magnetic data of the ship to that measured by the airborne magnetics. In areas without aeromagnetic profiles, a 500 km wide high-pass filter was applied.

### 2.3. Shipborne Gravity and Seismic Data

[15] A gravity meter installed on-board measured the ambient gravitational field at 1 Hz during the ANT-23/4 and ANT-26/3 expeditions. The gravity readings were drift corrected via onshore reference measurements at the beginning of the cruise ANT-26/3 in Wellington Harbor, New Zealand, and at the end of the cruise in Punta Arenas, Chile [Gohl, 2010]. Gohl [2007] processed the gravity data of the cruise ANT-23/4 in the same manner. A median filter with a 5 km window size was applied to remove heave variability.

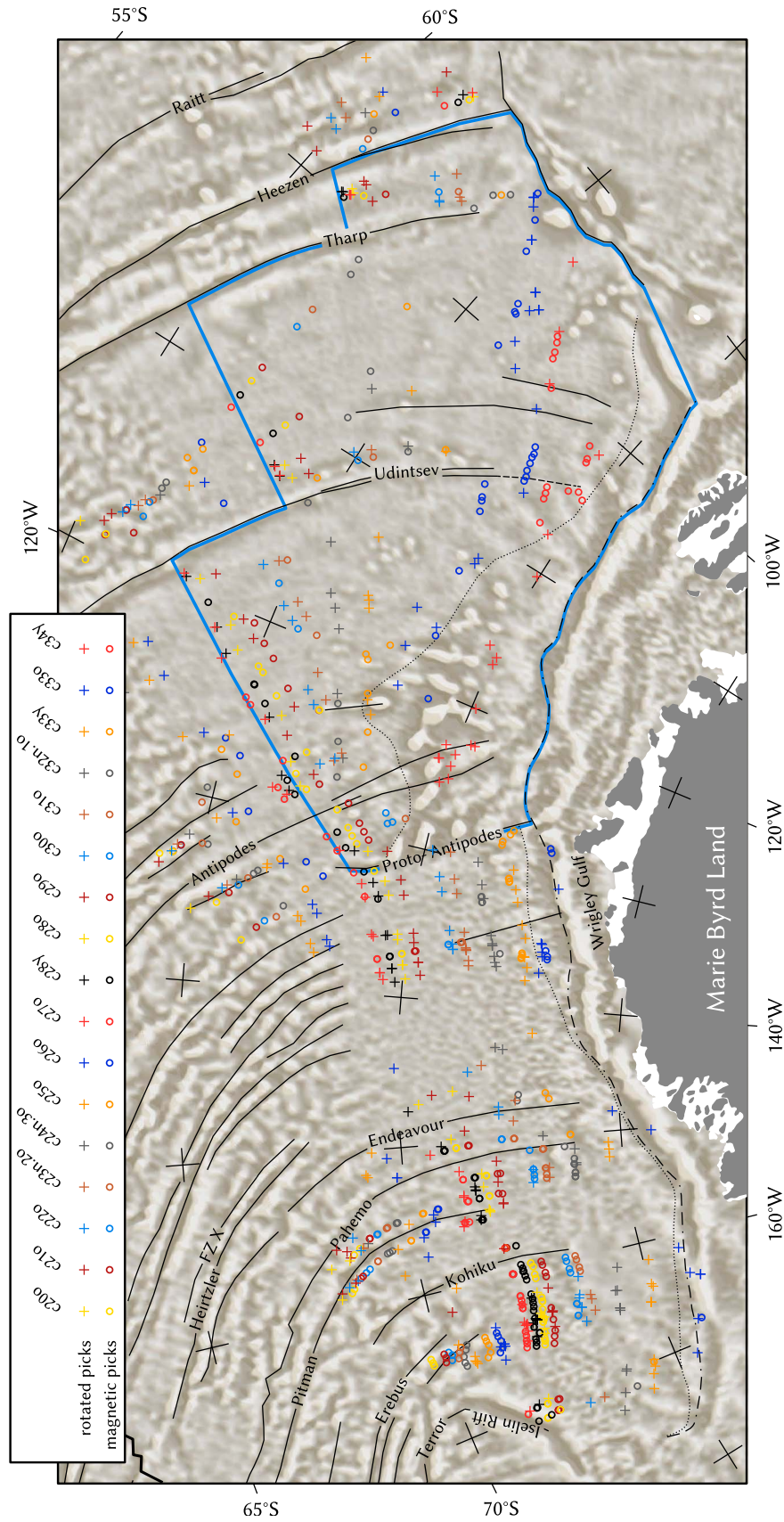
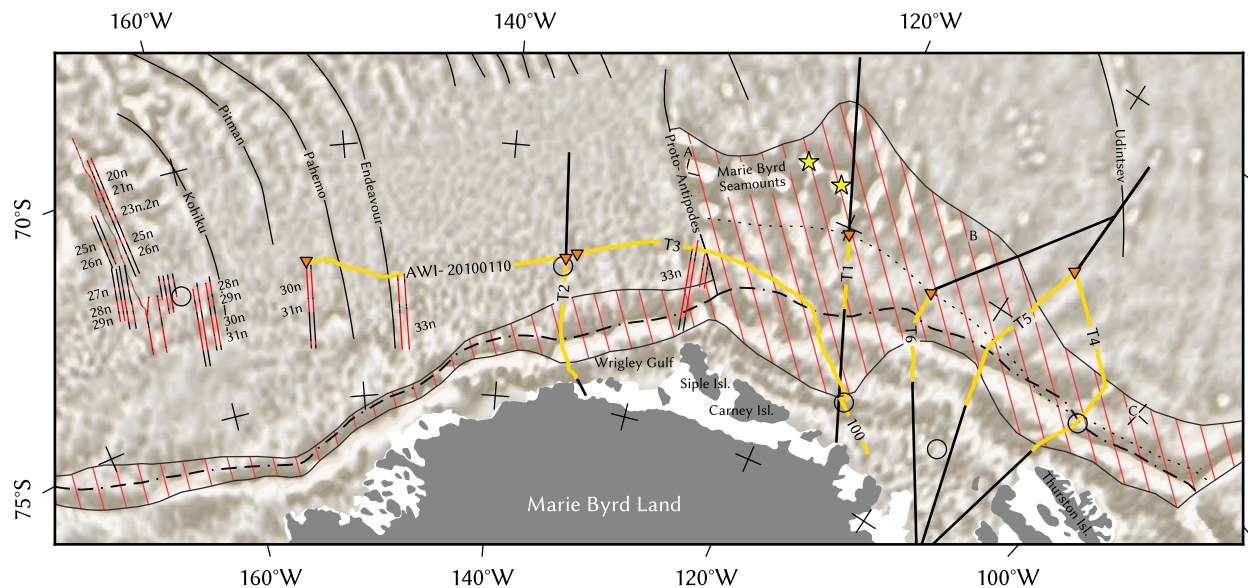


Figure 5



**Figure 6.** COTZ (striated) with reconstructed pre-rift suture (dashed line); calculated pre-rift suture, disregarding crustal addition (dotted line); seismic transects (thick yellow lines; 100 – AWI-20060100; T1 – AWI-20060200; T2 – AWI-20100111, AWI-20100112, AWI-20100113; T3 – AWI-20100117, AWI-20100118, AWI-20100119; T4 – AWI-20100126, AWI-20100129, AWI-20100130; T5 – AWI-20100131, AWI-20100132; T6 – AWI-20100139, AWI-20100140), and extensions (thick black lines); inverted triangles mark origin of each transect in Figure 7; identified magnetic spreading anomalies along ship profile ANT-2010S-03, and helicopter-magnetic lines (red – normal polarity, black – reversed); fracture zones (thin black lines); magnetic compensation loops (circles); A, B, C – see Figure A.VII in Text S1 in the auxiliary material; stars — locations of Haxby and Hubert Miller Seamount (from west to east). Base map: DNSC08 satellite gravity [Andersen and Knudsen, 2009], Lambert conformal conic projection with central meridian 145°W and standard parallels 74°S and 66°S.

[16] Deep crustal seismic refraction profiles, AWI-20060100 [Gohl *et al.*, 2007] and AWI-20060200 [Gohl, 2007; Lindeque and Gohl, 2010], acquired during the ANT-23/4 cruise in 2006, and a series of multichannel seismic reflection profiles, obtained during the ANT-26/3 cruise in 2010, lie within our study area (yellow lines in Figure 6). These seismic reflection profiles are currently being processed in-house (T. Kalberg, A. Lindeque, G. Uenzelmann-Neben, and E. Weigelt, personal communication, 2011). The most relevant parameters for this study, basement depth, seafloor and total sediment thickness, were picked in two-way-travel time (TWT) from the preliminary single channel seismic data. The TWT values were converted to depth (in km) using the sediment layer interval velocities from the finer AWI-20060200 P-wave refraction model [Lindeque and Gohl, 2010], and velocities for the deeper crust were obtained from both the AWI-20060100 and AWI-20060200 models. The

converted basement depths and total sediment thicknesses were incorporated in the gravity model.

### 3. Models

#### 3.1. Magnetic Modeling

[17] The first step in our modeling was to identify the marine magnetic spreading anomalies along our profiles. This was done based on the methods and techniques of Vine and Matthews [1963]. The synthetic spreading models were calculated using the open-source program MODMAG [Mendel *et al.*, 2005], applying the geomagnetic polarity timescale of Gradstein *et al.* [2004]. Two magnetic GEODAS profiles (Figure 1), EW9201 (R/V Maurice Ewing, 1992) and NBP96-2 (R/V Nathaniel B. Palmer, 1996), served as reference to tie the newly acquired aeromagnetic data to existing Pacific–Antarctic spreading models [Cande *et al.*, 1995; Croon *et al.*, 2008].

**Figure 5.** Compilation of magnetic picks on the West Antarctic and Bellingshausen plate, and rotated picks from the Pacific plate used for plate-tectonic reconstruction. Fracture zones (black lines); pre-rift suture (dashed line); COB (dotted line); and Bellingshausen plate (blue outline). Base map: DNSC08 satellite gravity [Andersen and Knudsen, 2009], Lambert conformal conic projection with central meridian 145°W and standard parallels 72°S and 60°S.

[18] Helicopter- and ship-magnetic lines, obtained during the Polarstern cruise ANT-26/3, and GEODAS lines NBP94-2 and NBP9702, included in the existing model, increased the density of the magnetic spreading anomaly picks in the eastern Ross Sea and western Amundsen Sea. Figures 1–5 show the identified magnetic spreading anomalies from all available datasets (see auxiliary material for additional data).<sup>1</sup>

### 3.2. Gravimetric Modeling

[19] Since refraction models in the area are sparsely distributed, gravity modeling was used to further estimate the crustal thickness, location of the continent–ocean boundary (COB) and width of the COTZ. We chose six transects from the continental shelf break to the abyssal plane, all approximately perpendicular to the continental shelf, so as to cross the potential COB and COTZ optimally (Figure 6). Lines reaching beyond the continental shelf were extended with satellite-derived gravity data [Andersen and Knudsen, 2009], bathymetry data [Andersen and Knudsen, 2009] and sediment thickness values [Scheuer *et al.*, 2006]. The seafloor and basement depth, as well as total sediment thickness from the 2010 seismic reflection data, were imported in the gravity model as fixed layers. Where available, on-board gravity and echosound bathymetry data were used to supplement the seafloor picked in the single channel seismic data. The gravity response was then calculated by forward modeling using the method of Watts [1988] and Watts and Fairhead [1999]. We estimated densities of sedimentary rocks from P-wave velocities according to Gardner *et al.* [1974] and assumed uniform densities for the upper crust, the lower crust and the mantle on all transects to obtain crustal models. Then we created a start model that is similar to the deep crustal profile (T1) and tried to fit the measured gravity by altering the structure of the crust as little as possible. When the thickness of the sediments overlying the basement is known from seismicity we did not change them. Fortunately, the geometry of the sediments and water column have the biggest influence on the gravity signal, so there is less freedom for fitting the underlying crust in the model.

[20] The resulting gravity models (examples T1 and T2 in Figure 7) constrained the pre- and post-rift crustal thickness well, allowing us to assess the amount of continental deformation involved during

the initial rifting process and subsequent Zealandia–Antarctica breakup.

### 3.3. Continental Deformation Model

[21] Our model considers deformation that is located in the COTZ (stippled area in Figure 8), an area, where the origin of the crust cannot be classified unequivocally as either continental or oceanic. In this zone, oceanic crust can be interleaved with segments of transitional crust, but the crustal thickness generally increases from its outer edge to the inner bound. Contrary, the amount of generated melt increases towards the outer edge, where the thickness of the oceanic crust equals the melt thickness.

[22] In order to reconstruct the pre-rift shape of the Marie Byrd Land margin, we determined the width of the COTZ,  $l_e$ , and the crustal thickness prior to its extension,  $t_0$ , within each of the six seismic transects T1 to T6. We assumed volume constancy of the continental crust during deformation, and—reduced to a 2D profile—a continuous cross section area,  $A_c$ .

[23] The aforementioned parameters permitted the calculation of the pre-rift width of the COTZ,  $l_0$ , the mean thickness of the extended crust,  $t_r$ , and the stretching factor,  $\beta$ , according to the equations in Figure 8. Both,  $t_r$  and  $\beta$ , are independent from the obliquity of the 2D section with respect to the COTZ, when a three-dimensional continuation of the geological units to either side of the 2D section is presumed. The areal extent of the COTZ, depicted in Figures 1 and 6, was estimated by interpolation between the seismic transects.

### 3.4. Plate–Tectonic Reconstruction

[24] Visual fitting of picks of the magnetic spreading anomalies from Cande *et al.* [1995], Eagles *et al.* [2004b], and this study as well as fracture zone traces using GPlates [Boyden *et al.*, 2011] yielded new finite rotations (Figure 5; see also Figure A.IV and Table B.I in Text S1 in the auxiliary material).

[25] Occasionally, ambiguities in the magnetic identifications allowed for multiple rotation solutions. In these cases, we regarded the position of flow lines and fracture zones to be more trustworthy than the location of modeled magnetic isochrons and preferred a better fit of flow lines over that of magnetic isochrons. Fracture zones were digitized from seismic lines and satellite gravity data. Lateral shifts of magnetic identifications in adjacent

<sup>1</sup>Auxiliary materials are available in the HTML. doi:10.1029/2011GC003742.

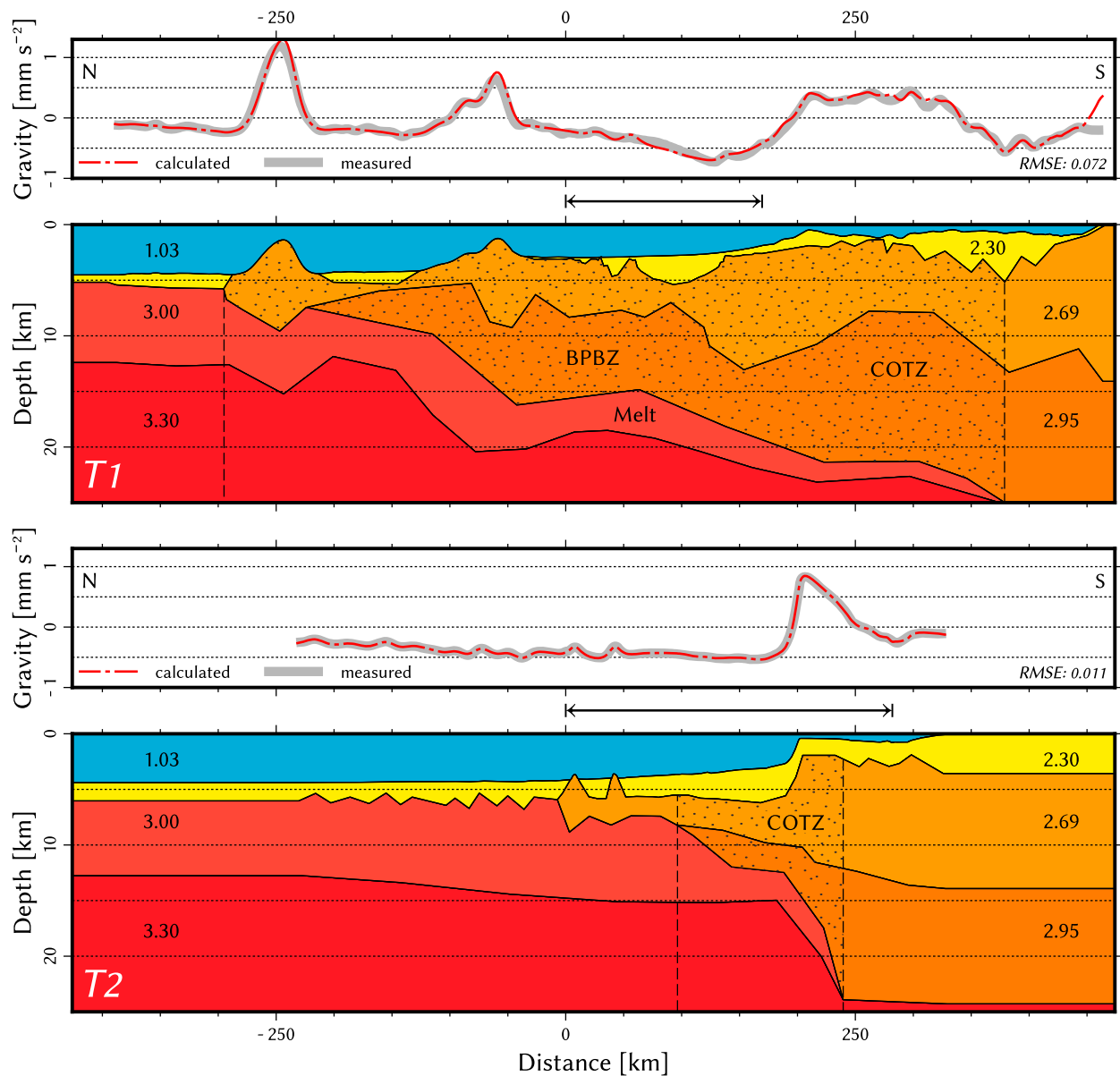


**Figure 7.** Crustal models along seismic transects T1 and T2 (locations on map in Figure 6). Numbers in the cross-section represent density ( $\text{g cm}^{-3}$ ); stippled area indicates extended transitional crust/Bellingshausen Plate Boundary Zone (COTZ/BPBZ). Arrows indicate area covered by seismic transect. Transects T3 to T6 in auxiliary material.

profiles further constrained fracture zone traces that are not apparent as flow lines in the gravity data.

[26] Whenever magnetic data were unavailable due to the Cretaceous Normal Superchron (84–125 Myr) or tectonic/magmatic overprinting, we attempted to determine the finite rotation pole by extrapolating spreading rates from the oldest distinguishable chron back to the margin. For this we assumed that spreading rates were constant during the Cretaceous Normal Superchron and resembled the rate that was determined at c34y (84 Myr). In some cases, it was possible to estimate the spreading rate directly

from existing spreading anomalies on the conjugate margin assuming identical half-spreading rates. The pre-rift reconstruction of Marie Byrd Land, Chatham Rise, and Campbell Plateau originated from the fit of the pre-rift sutures of the continental margins at 90 Myr.

## 4. Data Analysis and Discussion

### 4.1. Crustal Model

[27] The crustal models (Figure 7), obtained from gravity inversion along seismic transects T1 to T6

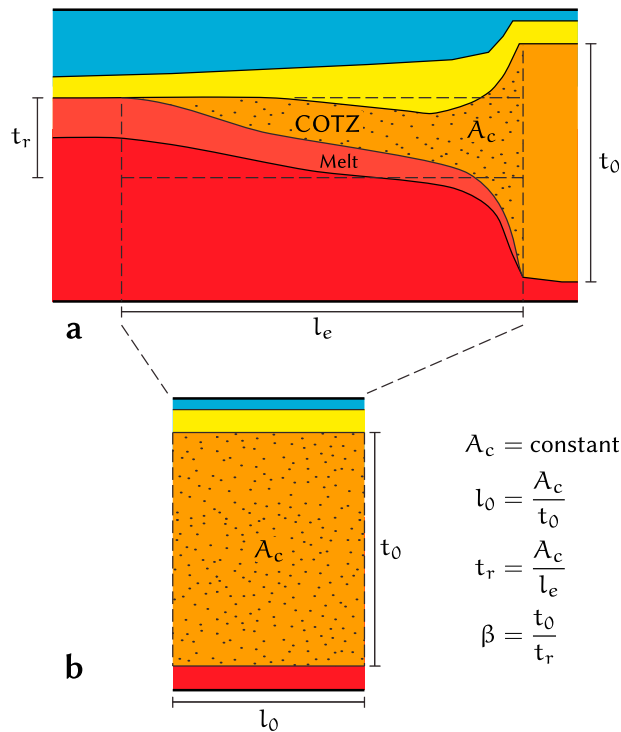


**Figure 8.** Determination of the COTZ width prior to rifting. (a) Extended transitional crust (stippled area) on passive continental margin from gravity inversion model (Figure 7). (b) Reconstruction of the stippled area in Figure 8a before rifting.  $\beta$  — stretching factor;  $A_c/l_e$  — COTZ area/width;  $l_0$  — pre-rift width of COTZ;  $t_0/t_r$  — initial/extended crustal thickness.

(Figure 6), image an uneven basement, covered by sediments up to 2.8 km thick. If we compare the top-of-basement of *Grobys et al.* [2009] with our crustal models, we observe a 1 km elevation difference between Zealandia and Marie Byrd Land, consistent with the findings of *Sutherland et al.* [2010]. The Moho depth varies around 24 km, and the lower crust is generally 10 km thick.

[28] Two representative crustal models along the seismic transects T1 and T2 are displayed in Figure 7. The models consist of five layers—sedimentary cover ( $2.3 \text{ g cm}^{-3}$ ), upper crust ( $2.69 \text{ g cm}^{-3}$ ), lower crust ( $2.95 \text{ g cm}^{-3}$ ), melt addition/oceanic crust ( $3.0 \text{ g cm}^{-3}$ ), and mantle ( $3.3 \text{ g cm}^{-3}$ )—whose densities and thicknesses were obtained from the velocity–depth model.

[29] Apart from slight deviations, the gravity-derived crustal model of transect T1 reflects the observations from the velocity–depth model: Crust with a low density, but anomalously large thickness extends seaward of the continental slope. The Moho and the boundary between upper and lower

crust rise gradually towards the shelf, and the gravity anomaly describes the rugged topography of the upper crust and the Marie Byrd Seamounts. The upper part of the submarine volcanoes consists of material with approximately equal density as the upper crust. Subsidence of the transitional crust and subsequent formation of small sediment basins increase the distance of the denser material to the surface and generate negative gravity anomalies.

[30] By contrast, transect T2, which lies west of the Marie Byrd Seamounts, displays an elongated positive free-air gravity anomaly aligned with the Moho step. This anomaly is caused by gravimetric superposition of the Moho step with the bathymetric step of the steep continental slope and some minor sedimentary effect. The gravity high is followed by a less pronounced landward low close to the shelf that trends subparallel to shelf edge. Comparable elongate gravity anomalies are considered commonly associated with Atlantic-type passive continental margins [*Watts, 1988; Watts and Fairhead, 1999*]. Unlike T1, the transition from thick continental crust to thin oceanic crust is abrupt with the Moho raising about 8 km. The sedimentary cover reaches thicknesses of up to 4 km.

[31] Transects T3 to T6 (see auxiliary material) are more similar to transect T1 than to T2. The former transects feature an equally thick low-density crust extending far from the slope. The free-air anomaly, also similar to that in the transect T1, indicates the same rugged crust topography and sedimentary cover. Compared to the cross sections further west, transects T4 and T5 are characterized by increased amounts of sediments (3–4 km) on the slope. We observed a small but distinct increase of the upper crust thickness, where transect T3 crosses the Proto-Antipodes Fracture Zone.

[32] Except for the central part of transect T1, which is covered by the velocity–depth model, the gravity models are based only on reflection seismic data. This leads to lower confidence on sediment thickness estimates due to poorly constrained interval velocity, as well as a lack of information about basement properties. However, variations of sediment and basement properties within commonly-accepted bounds would not be enough to explain the gravity field differences between the transects. Hence, we expect the effects of these uncertainties on the determination of the crustal thickness, COTZ, and  $\beta$ -factors to be small.

[33] We can distinguish between the Marie Byrd Land sector with a sharp transition in the free-air

**Table 1.** COTZ Properties of the Marie Byrd Seamount Province Along Seismic Transects (Figure 6)

Number	$\beta$ -Factor	COTZ Width	Cont. Stretching
T1	1.83	670 km	304 km
T2	2.62	145 km	90 km
T3	—	—	—
T4	1.89	225 km	106 km
T5	3.55	220 km	158 km
T6	3.12	345 km	234 km

anomaly and a narrow COTZ, and the extremely wide Bellingshausen Plate Boundary Zone (BPBZ).

[34] The Marie Byrd Land margin best compares to magma-poor passive continental margins in the central South Atlantic, e.g., the Brazilian Espírito Santo margin and conjugate North Angolan margin [Blaich *et al.*, 2011; Huismans and Beaumont, 2011]. Despite the uncertainties in the crustal models, several features support this classification: There are no indications of syn-rift magmatism like oceanic seaward dipping reflectors or anomalously high P-wave velocities within the transitional crust. Instead, seismic velocities of the lower crust [Gohl *et al.*, 2007; Gohl, 2007; Lindeque and Gohl, 2010] are consistent with magmatic underplating. Throughout the entire Marie Byrd Land margin, we observed a wide region of thinned transitional crust of low density. Sedimentation patterns in the seismic image of line AWI-20100110 reveal sedimentation patterns of a type similar to those observed off the southeastern Brazil–Angola margin (A. Lindeque, personal communication, 2011). Unlike the Marie Byrd Land sector, the Bellingshausen sector is unique in that it was subject to ongoing deformation and volcanism after breakup. This is further discussed in section 4.5.3.

[35] Close to the Antarctic shelf—where thick sediment layers attenuate the gravity signal of the basement—flow lines, indicating fracture zones, cannot be traced anymore. On the seismic image of line AWI-20100110, the basement reflectors are discontinuous and show a vertical offset of 0.2–0.3 s TWT. These features are interpreted as spatially coincident fracture zones, which are also evident in the bathymetry (A. Lindeque, personal communication, 2011), and correspond to the magnetic anomaly signatures in our study (Figure 6). The seismic transect and observed shifts in the magnetic pattern between parallel magnetic profiles along the Kohiku Fracture Zone support the proposed position and extend the fracture zone

interpretation further south. We further constrained the locations of Pahemo and Endeavour Fracture Zones at their southern tips from seismics and magnetic spreading anomalies (Figure 1).

## 4.2. Continental Extension of Marie Byrd Land

[36] We identified domains of transitional crust, illustrated as stippled areas in the cross-sections in Figure 7, along each of the six crustal models T1 to T6. Consequently, the area representing the present-day COTZ was determined by interpolation between the transects (striped area in Figure 6). We derived the parameters  $A_c$ ,  $t_o$ ,  $t_r$  and  $l_e$  from the cross-sections and calculated the (along-profile) pre-rift width of the COTZ, the pre-rift suture as well as the amount of continental stretching and the associated stretching factors ( $\beta$ ) according to the scheme in Figure 8. The results, summarized in Table 1 and Figure 6, indicate a strong regional variation of the COTZ width. The width of the COTZ steps from 50–130 km west of the Proto-Antipodes Fracture Zone to more than 650 km east of that fracture zone. By contrast, the stretching factors remain low to moderate (1.8–3.5) on the entire Marie Byrd Land margin.

[37] We determined the amount of generated melt along the transects to obtain unbiased  $\beta$ -factors by fitting the gravity anomalies with an extra underplate layer. This layer gradually increases in thickness from its inner (continental) bound to the outer (oceanic) side, where it eventually transforms into oceanic crust. There is not much room for big melt thickness and initial crustal volume variability in fitting transect T2 so that we can assume a constant volume of the deformed crust. The estimation of added material due to volcanism in the Marie Byrd Seamount province remains speculative with the available data. Therefore, fitting Chatham Rise to Marie Byrd Land can only be attempted via the plate circuit West Antarctica–Campbell Plateau–Chatham Rise–Bellingshausen plate.

[38] The initial crustal thickness of 20–24 km for Marie Byrd Land is equivalent to the thickness of the submarine plateaus of Zealandia [Grobys *et al.*, 2009, and references therein]. Further, the crustal thickness model of Grobys *et al.* [2008] suggests a mean COTZ width of 100 km for the Campbell Plateau and Chatham Rise. Although these widths are similar to those on the western Marie Byrd Land margin, they differ much from those of the eastern part of Marie Byrd Land, which raises the question

whether extensive continental stretching was associated with rifting only (see section 4.5.3).

### 4.3. Age and Spreading Model

[39] We identified magnetic spreading anomalies along 44 helicopter- and ship-magnetic profiles in the eastern Ross Sea (Figures 1–5). Both data sources show clearly identifiable seafloor spreading anomalies with similar amplitudes (Figure A.IX in Text S1 in the auxiliary material), even though the shipborne data are preprocessed more aggressively.

[40] The oldest identified magnetic spreading anomaly, c33n (73.6–79.5 Myr), occurs in several locations in the Ross Sea, the Wrigley Gulf and to the west of the Marie Byrd Seamounts/Proto-Antipodes Fracture Zone (Figure 1). A reversed magnetic anomaly occurs south of c33n. Based on its proximity and location within the COTZ, it is more likely to be of continental origin than a c33r magnetic seafloor spreading anomaly.

[41] The spreading model in Figure A.VIII in Text S1 in the auxiliary material suggests a half-spreading rate of about 30 mm yr<sup>-1</sup> along the Pahemo Fracture Zone during c32n.2n (72 Myr). Later, the spreading rate increased up to 37 mm yr<sup>-1</sup>, where it peaked around chron c27n, and steadily decreased to 11 mm yr<sup>-1</sup> between chrons c26n and c22n. Further west, the spreading rate was slower by about 10 mm yr<sup>-1</sup> (Figure A.IX in Text S1 in the auxiliary material).

### 4.4. Fitting Fracture Zones

[42] Fracture zones and flow lines in the South Pacific (Figure 5; see also Figure A.IV in Text S1 in the auxiliary material) are essential constraints for the lateral alignment of conjugate plates in the plate-tectonic reconstruction (Figure 9; see also Figure A.V in Text S1 in the auxiliary material). Although fracture zones prior to 43 Myr are explained well by synthetic flow lines derived from the models of *Cande et al.* [1995], *Larter et al.* [2002], and *Eagles et al.* [2004a], the fit of older fracture zones of conjugate plates is not ideal. There are particularly large model differences during the initial rifting phase between Zealandia and Marie Byrd Land. We suspect this to be due to fitting unreliable or not well constrained magnetic isochrons using the *Hellinger* [1981] criteria [*Cande et al.*, 1995; *Larter et al.*, 2002]. In this study, we improved the plate-tectonic reconstruction by visually fitting magnetic picks and fracture zones

while ensuring that the model would be geologically sound (Figure 5; see also Figure A.V in Text S1 in the auxiliary material).

[43] Fracture zones, as observed in satellite gravity, are generally 10 km wide and have clearly defined boundaries in the gravity signal. We assume that we can achieve an accuracy of about 2 km if we take care to digitize the same boundary or the centerline on both conjugate plates. As there are many parallel fracture zones along the margin, these errors average out in the end. We determined the offsets between conjugate fracture zone segments in the Ross Sea sector using the rotation poles of *Eagles et al.* [2004a], and compared these results to the offsets in our model. We obtained a general misfit of considerably less than 5 km, whereas offsets as large as 60 km occur in the former model.

### 4.5. Plate-Tectonic Reconstruction

[44] In Figure 9, we present the key frames of the improved plate-tectonic reconstruction of the conjugate Marie Byrd Land and Zealandia margins. *Croon et al.* [2008] refined the Pacific–Antarctic plate rotations of previous studies by *Cande et al.* [1995], *Cande and Stock* [2004], and *Eagles et al.* [2004a], however, their model does not include rotations prior to c20o (43 Myr). Here, we focus on the evolution of Marie Byrd Land and Zealandia beyond that point. An animation included in Text S1 in the auxiliary material shows the deduced plate movements, which could be divided into the following major phases of plate reorganizations:

[45] *90–84 Myr (c34n)* Onset of continental extension; Chatham Rise separated from Marie Byrd Land as a fragment of Zealandia with a velocity of 30–40 mm yr<sup>-1</sup>. Rifting started in the Amundsen Sea, where the oldest seafloor spreading anomalies (c34y) are observed, and then propagated west.

[46] *84–80 Myr (c33r)* Zealandia and Marie Byrd Land initially rotated about a pole located in Wilkes Land; spreading propagates into the Ross Sea.

[47] *84–62 Myr (c33r–c27r)* The Bellingshausen plate moved as an independent plate for about 22 Myr. During this time, the southern plate boundary was subject to extensive transtension located in an up to 670 km wide deformation zone.

[48] *80–74 Myr (c33n)* The Campbell Plateau and Chatham Rise rotated against each other and the Bounty Trough was opened. The Bollons Seamount was transferred to the southeastern plate

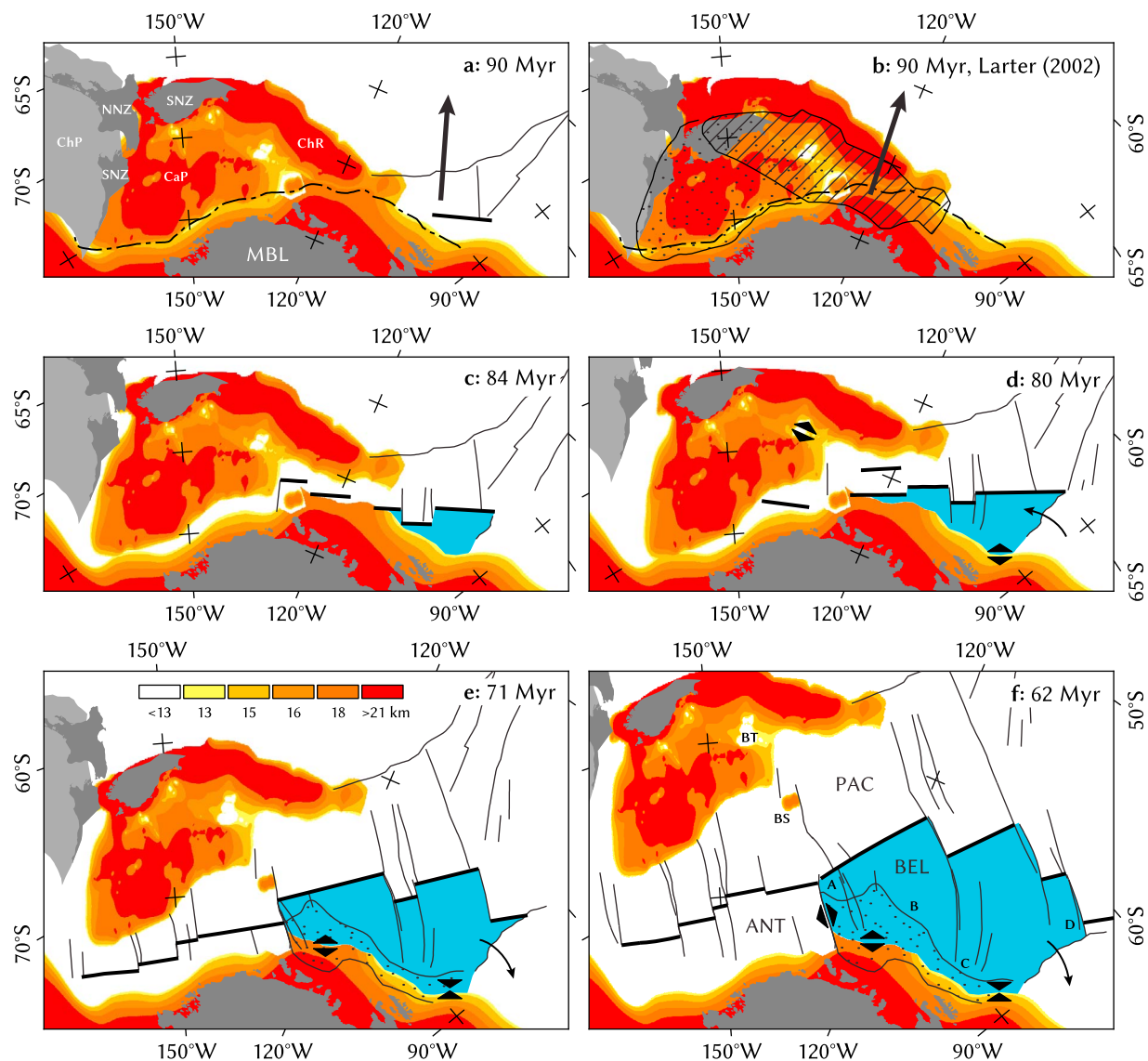


**Figure 9.** Pre-rift reconstruction models of Marie Byrd Land, Chatham Rise, and Campbell Plateau (a and c–f) using finite rotations of this study and from *Grobys et al.* [2008], and (b) using rotation parameters from *Larter et al.* [2002] and *Eagles et al.* [2004a]. Chatham Rise (striated), Campbell Plateau (stippled), and Marie Byrd Land overlap the pre-rift suture (dashed line) from this study. Arrows indicate initial plate motion direction of Pacific plate/Chatham Rise. Plate-tectonic reconstruction models of Zealandia, Marie Byrd Land, and Bellingshausen plate (Figures 9c–9f) at magnetic chrons c34y (84 Myr), c33o (80 Myr), c32n.1o (71 Myr), and c27o (62 Myr). The Bellingshausen plate (blue) moved independently from the Antarctic plate between c34y and c27o (small arrows). Oceanic crust formed along the southern Bellingshausen plate margin (Figures 9c and 9d) was later deformed (BPBZ, stippled area, Figures 9e and 9f). The tectonic regime in the BPBZ and Bounty Trough is illustrated by arrowheads pointing towards (convergent) and away (divergent) from each other. The Bollons Seamount was transferred from the West Antarctic to the Pacific plate around c33o. The rotation between Chatham Rise and Campbell Plateau occurred during chron c33n. Parallel spreading centers at 120°W (Figure 9d) represent ridge jumps. Thin black lines — fracture zones, thick black lines — mid-ocean ridge segments; ANT — West Antarctic plate, BEL — Bellingshausen plate, BS — Bollons Seamount, BT — Bounty Trough, CaP — Campbell Plateau, ChP — Challenger Plateau, ChR — Chatham Rise, MBL — Marie Byrd Land, NNZ — North Island of New Zealand, PAC — Pacific plate, SNZ — South Island; A, B, C, D — see Figure A.VII in Text S1 in the auxiliary material. Base map: crustal thickness of Zealandia [*Grobys et al.*, 2008] and Antarctica, Lambert conformal conic projection with central meridian 145°W and standard parallels 72°S and 60°S.

boundary of the Campbell Plateau. The lateral displacement between Marie Byrd Land, Campbell Plateau and Chatham Rise was shifted from the Bollons transform fault west of Bollons Seamount to the Proto-Antipodes Fracture Zone. Plate motion velocities between Marie Byrd Land and Zealandia ranged from 50 (west of the Proto-Antipodes Fracture Zone) to 80 mm yr<sup>-1</sup> (east of the Proto-Antipodes Fracture Zone). The tectonic regime in the Ross Sea changed from transtension to extension, and first fracture zones were formed.

[49] 74–62 Myr (c32r.2r–c27r) The rotation between Campbell Plateau and Chatham Rise ceased, and the Pacific–Antarctic separation velocity decreased to 55–70 mm yr<sup>-1</sup>. The rotation of the Bellingshausen plate shifted from counterclockwise to clockwise (Figure A.VII in Text S1 in the auxiliary material), causing a characteristic curve in the trace of the Udintsev Fracture Zone and the Eltanin Fault System. Eventually, the independent motion of the Bellingshausen plate stopped around 62 Myr, and the plate became fixed to the West Antarctic plate.

[50] 71–69 Myr (c31r) The traces of the Pahemo, Endeavour, and Kohiku Fracture Zones begin to bend left in direction from the Ross Sea towards the spreading center, indicating a slight shift of the Pacific plate motion direction. The Bollons Seamount passed the northern tip of the Proto-Antipodes Fracture Zone during the same time, and the overall spreading velocity decreased by about 10 mm yr<sup>-1</sup>.

[51] 62–45 Myr (c26r–c21n) Following the end of the independent Bellingshausen plate movement, full-spreading rates constantly decreased from 60–70 mm yr<sup>-1</sup> to 30–40 mm yr<sup>-1</sup>.

[52] 45–42 Myr (c20r–c20n) For a short period, the rotation pole between the West Antarctic and Pacific plates moved into the Ross Sea (163°49.8'W, 71°17.4'S) and initiated a 3.5° counterclockwise rotation of the Pacific plate relative to West Antarctica in only 3.8 Myr.

#### 4.5.1. Estimation of Breakup Time

[53] The time of onset of the COTZ formation is not constrained by our observations, but we interpret the margin west of the Proto-Antipodes Fracture Zone as forming during c33r and the end of c33n (79.5 Myr). Supporting our interpretation, *Siddoway et al.* [2004] relate a rapid cooling event during 80–71 Myr—recorded by apatite fission-track ages of samples from the Cape Colbeck region in

the Eastern Ross Sea—to denudation associated with the breakup of Campbell Plateau from Marie Byrd Land.

[54] Breakup time estimates in the range of 105–81 Myr in earlier works [e.g., *Molnar et al.*, 1975; *Cande et al.*, 1995; *Luyendyk*, 1995; *Larter et al.*, 2002; *Stock and Cande*, 2002; *Cande and Stock*, 2004; *Eagles et al.*, 2004a] are based on paleomagnetic data or extrapolation of spreading rates back into the Cretaceous Normal Superchron (c34n). Without the benefit of dated samples from the margin or magnetic anomalies of the appropriate age, the onset of COTZ formation and the initial rate of COTZ deformation are basically unknown, but likely fall within a certain range of possibilities.

[55] The new magnetic data we collected in vicinity of the Proto-Antipodes Fracture Zone indicates that Chatham Rise and Campbell Plateau separated from Marie Byrd Land with a velocity of 30–40 mm yr<sup>-1</sup> during chron c33r (79.5–84 Myr). These velocities also match spreading rates based upon extrapolation beyond the oldest chrons detected along the margin west of the Proto-Antipodes Fracture Zone.

[56] Taking into account the continental deformation (~90 km extension along the margin of Campbell Plateau and Marie Byrd Land) during breakup and assuming a constant spreading rate during chrons c33r and c34n, a close fit of the modeled pre-rift suture between Zealandia and West Antarctica is reached at about 89 Myr. Subduction of the Hikurangi Plateau beneath the Chatham Rise stopped around 96 Myr [*Davy et al.*, 2008]. Aside from maybe back-arc extension before that time, we consider this to be the earliest possible onset of the Zealandia–Antarctic rifting with an implied minimal plate motion velocity of 14 mm yr<sup>-1</sup> during the rifting phase.

[57] Numeric lithosphere extension models suggest that the rifting time—before continental breakup occurs—is a function of extension velocity [*van Wijk and Cloetingh*, 2002]. For rapid breakup times (in this case 5–12 Myr with an initial extension between 96 and 89 Myr), their models predict extension rates of more than 30 mm yr<sup>-1</sup>.

[58] Although the crustal thickness of the modeled crust is greater than that of the Marie Byrd Land margin and the rheology of the latter is unknown, which could alter the relationship between rifting time and extension velocity, we nevertheless attempted to estimate the breakup time based on the data of *van Wijk and Cloetingh* [2002]. In our

reconstruction, a late extension (starting at 90 Myr and with a separation velocity of  $>30 \text{ mm yr}^{-1}$ ) as opposed to an earlier extension (at 96 Myr with a slower velocity of about  $14 \text{ mm yr}^{-1}$ ) fits the *van Wijk and Cloetingh* [2002] model better.

#### 4.5.2. Early Breakup and Opening of Bounty Trough

[59] New evaluation of continental extension on the Marie Byrd Land margin in this study and the crustal thickness model of *Grobys et al.* [2008] have enabled numerous improvements to the reconstruction of the early Zealandia–Marie Byrd Land breakup history. Also they provided answers to open questions and voids of previous studies that originated from a lack of constraints regarding the dynamics of the plate margins.

[60] Unresolved issues remaining in previous reconstructions include:

[61] 1. The rotation of Chatham Rise with respect to Campbell Plateau by *Larter et al.* [2002] causes a 350 km wide overlap because the extend of the COTZ on both margins was underestimated. This close fit reconstruction of Marie Byrd Land and Chatham Rise introduces an overlap of the latter with the continental shelf of Marie Byrd Land as far as Siple and Casey Islands (Figure 9b). Further, the Bollons Seamount is traversed by Chatham Rise, and the southwest margin of Campbell Plateau overlaps the continental shelf of the West Antarctic Plate by about 100 km. A compression of this dimension cannot be explained by our continental deformation model, since the transitional crust of the continental shelf of Marie Byrd Land, the crust of the Bounty Trough, and its adjacent plateaus [*Grobys et al.*, 2008] is relatively thick (low  $\beta$ -factors).

[62] 2. *Davy et al.* [2008] interpreted the cessation of subduction of the Hikurangi Plateau beneath the Chatham Rise at about 96 Myr, followed by a switch in the tectonic regime in New Zealand from northeast to northwest directed extension, which *Davy et al.* [2008] construed to be parallel to the breakup orientation. The southern branches of Udintsev and adjacent Fracture Zones further east (Figure 5; see also Figure A.IV in Text S1 in the auxiliary material) strike northwest–southeast, thus confirming a northwest directed separation of Chatham Rise from Marie Byrd Land. *Larter et al.* [2002] and *Eagles et al.* [2004a] suggest a north by west directed initial movement of Chatham Rise (90–84 Myr, arrow in Figure A.VI and supporting

animation in Text S1 in the auxiliary material) which is oblique to the fracture zones and contradicts the interpretation of *Davy et al.* [2008].

[63] Our updated plate reconstruction, based on the location of the pre-rift suture between Marie Byrd Land, Chatham Rise, and Campbell Plateau, ensures that there are no or only minor overlaps between Marie Byrd Land and Zealandia as well as Chatham Rise and Campbell Plateau. Further drawbacks of previous reconstructions were circumvented in this study by first rotating Zealandia with respect to Marie Byrd Land and then rotating Chatham Rise with respect to Campbell Plateau in a separate step, after the Bollons Seamount was transferred to the margin of the Campbell Plateau at about 80 Myr. This allowed a fit of the conjugate ends of the Udintsev Fracture Zone as well as adjacent fracture zones further east and guaranteed a northwest directed extension in New Zealand.

[64] The plate-tectonic reconstruction of Zealandia [*Grobys et al.*, 2008] does not constrain the time and duration of the rotation between Chatham Rise and Campbell Plateau. However, a rotation is not possible prior to chron c33n without introducing a cycle of rapid extension followed by compression along the southern boundary of the Bellingshausen plate (see animations in Text S1 in the auxiliary material). Furthermore, the reliability of the c34y identifications in the Bounty Trough area is questionable [*Davy*, 2006]. Rifting on the northern Campbell Plateau was complete by 84 Myr [*Cook et al.*, 1999], but the age of cessation of rifting is unconstrained for the Bounty Platform or southern Campbell Plateau. *Sutherland* [1999] suggests that a ridge may have existed during c33n in the outer part of the Bounty Trough and then jumped southward. By initiating the rotation between Chatham Rise and Campbell Plateau during chron c33n (as opposed to c34n [*Larter et al.*, 2002]), we can fit c33o south of Bollons Seamount while minimizing the Bellingshausen plate motion relative to Marie Byrd Land at the same time. This implies that until c33y, when the Chatham Rise vs. Campbell Plateau rotation ceased, the Proto-Antipodes Fracture Zone separated two independent spreading centers (Antarctic–Pacific and Antarctic–Campbell Plateau).

#### 4.5.3. Transitional Crust of the Bellingshausen Plate

[65] In section 4.2, we concluded that pre-rift crustal thicknesses of Marie Byrd Land, Campbell Plateau, and Chatham Rise were alike. Moreover,

the width of the COTZ of west Marie Byrd Land, Campbell Plateau, and Chatham Rise were uniform, whereas the BPBZ is three to five times wider (Figures 6 and 7 and Table 1). Because the opening of the Amundsen Sea and Ross Sea propagated from east to west, leading to lower spreading velocities in the west and increasing the potential of basin propagation [van Wijk and Cloetingh, 2002], we should expect a widening of the COTZ towards the Ross Sea. By contrast, we observed a narrow COTZ west of the Bellingshausen sector.

[66] There are several indicators implying that the extensive continental stretching between Chatham Rise and east Marie Byrd Land was not associated with the initial rifting alone, but instead developed partly after their separation:

[67] 1. Alkali basalt samples, dredged from Haxby Seamount and Hubert Miller Seamount (Figure 6) yield  $^{40}\text{Ar}/^{39}\text{Ar}$  ages ranging from  $64.73 \pm 0.84$  to  $55.72 \pm 0.63$  Myr [Kipf et al., 2008; A. Kipf et al., Seamounts off the West Antarctic margin of the Pacific: A case of non-hotspot intraplate volcanism, manuscript in preparation, 2012]. This dating clearly marks the end of the independent Bellingshausen plate movement and is too young to be associated with the rifting between Zealandia and Marie Byrd Land.

[68] 2. We determined an extension velocity of  $>30 \text{ mm yr}^{-1}$  (section 4.5.1) associated with a short rifting time. Continental deformation along the Campbell Plateau and western Marie Byrd Land margin ceased in less than 10 Myr, and lithosphere extension models [van Wijk and Cloetingh, 2002] suggest that deformation should have stopped in eastern Marie Byrd Land as well.

[69] 3. Magnetic spreading anomalies c34n, c33r, and partly c33n cannot be detected on the central Marie Byrd Land margin (Figure 5), although they exist on the conjugate margin (Chatham Rise). It is likely that oceanic crust formed on the Marie Byrd Land side as well and transformed later on.

[70] We propose that the complete Marie Byrd Land margin developed similar to the conjugate margin of Zealandia during the initial separation. Rifting between Chatham Rise and Marie Byrd Land stopped before c34y (84 Myr), and, consequently, oceanic crust formed in the Amundsen Sea. Most of this oceanic crust, generated on the Bellingshausen plate margin until the end of chron c33r, was either magmatically altered or tectonically interleaved with transitional crust at a 1:1 ratio.

[71] The Bellingshausen plate moved independently of the West Antarctic plate for about 22 Myr since c34y. Its plate motion trajectories indicate an overall plate drift to the northeast with respect to Marie Byrd Land and a velocity varying from 3 to  $36 \text{ mm yr}^{-1}$  with a peak around  $9 \text{ mm yr}^{-1}$  (Figure A.VII in Text S1 in the auxiliary material). The southern and western border of the Bellingshausen plate were subject to a  $8\text{--}14 \text{ mm yr}^{-1}$  dextral motion relative to Marie Byrd Land and subparallel to its plate boundary.

[72] First counterclockwise, then clockwise rotation of the Bellingshausen plate caused a tectonic regime of alternating convergence and extension west of the balance point B (Figure 9; see also Figure A.VII in Text S1 in the auxiliary material) and vice versa east of it. This is supported by previous studies by Larter et al. [2002], Cunningham et al. [2002], and Eagles et al. [2004b], who interpreted the Bellingshausen Gravity Anomaly (south-east of point C) and the continental margin off Thurston Island as zone of accommodated convergent motion between the Bellingshausen and West Antarctic plates. Seamounts occur en echelon along the southern plate boundary of the Bellingshausen plate near point A. Their strike is approximately northeast–southwest directed and perpendicular to the motion path of A during the second half of the existence of the autonomous Bellingshausen plate. The clockwise rotation, the strike of the seamount chains and the dated sample from Hubert Miller Seamount are indicators that the seamounts formed during the end of the independent Bellingshausen plate movement (65–55 Myr).

[73] Traditionally, the chemistry signal [Kipf et al., 2008, also manuscript in preparation, 2012], increased crustal thickness (Figure 7), local highs in the gravity field, and disrupted magnetic signature were used as indicators to suggest intraplate volcanism as a simple solution to account for the transitional crust in the Bellingshausen plate [e.g., Storey et al., 1999]. Our data, the geochemical signature, and the age of the Marie Byrd Seamounts [Kipf et al., 2008, also manuscript in preparation, 2012] indicate that the Bellingshausen plate motion preceded intraplate volcanism. The tectonic setting at the time the seamounts formed indicates an enriched mantle source [Halliday et al., 1995; Pilet et al., 2008], which released melts through fissures created by lithospheric extension on the southern Bellingshausen plate margin. Fertilization of the mantle could either be explained by Mesozoic

subduction beneath the Gondwana convergent margin or by metasomatism of the lithospheric mantle through fractures in the weakened Bellingshausen plate.

[74] Especially during chron c33r (79.5–84 Myr) and at the end of the existence of the plate, there was very little movement relative to Marie Byrd Land. Lithosphere extension models show that rifting velocities lower than  $8 \text{ mm yr}^{-1}$  do not lead to seafloor spreading because the lithosphere in the formed basin cools and becomes stronger than in the surrounding regions [van Wijk and Cloetingh, 2002]. Consequently, the deformation zone migrates and the process repeats itself, forming a wide COTZ. We assume, a similar process, combined with oscillating transpression and transtension along the Bellingshausen plate margin, lead to the formation of an up to 670 km wide zone of transitional crust interleaved with segments of oceanic crust (BPBZ, in Figure 7). The deformation was intense enough to annihilate signs of oceanic crust such as magnetic seafloor spreading anomalies.

## 5. Summary

[75] We present and analyze an extensive new dataset of air- and shipborne geophysical measurements acquired during R/V Polarstern cruises in 2006 (ANT-23/4) and 2010 (ANT-26/3) at the rifted oceanic margin of Antarctica in the eastern Ross Sea and Bellingshausen Sea. We construct models of seafloor magnetic anomalies to interpret oceanic age, and models of the continental margin crust that are constrained by active-source seismic reflection and refraction data as well as gravity data. We subdivide the continental margin into two sectors divided by the Proto-Antipodes Fracture Zone (Figure 6).

[76] The western sector of the continental margin, the Marie Byrd Land sector, has a relatively narrow steep slope and resembles a typical magma-poor margin. The width of the COTZ on our modeled transect is 145 km, which we interpret—based on our crustal model—to represent an initial continental crust of thickness 24 km and width 55 km. It was stretched 90 km and intruded at its base by melt, eventually transitioning to normal-thickness oceanic crust ( $\sim 7 \text{ km}$ ) [White *et al.*, 1992] at its seaward limit.

[77] The eastern sector of the continental margin, the Bellingshausen sector, is broad and complex with abundant morphologic evidence for later

volcanism, confirmed by dredging [Kipf *et al.*, 2008]. The widths of the COTZ/BPBZ on our modeled transects are up to 670 km, and substantial uncertainty remains as to the nature of the crust within the COTZ/BPBZ because we have little control on crustal thickness or density. Our preferred interpretation is that some stretched continental crust is present throughout this zone, but that it has been substantially added to by basaltic igneous rocks (density  $3.0 \pm 0.1 \text{ g cm}^{-3}$ ). The extension estimates fall in the range of 106–304 km for the COTZ/BPBZ (Table 1).

[78] We identify seafloor magnetic anomalies c33n (79.5 Myr) to c20n (42 Myr) on a number of transects adjacent to the Marie Byrd Land sector (Figures 1–5). The Bellingshausen sector is too complex and sparsely sampled for us to reliably interpret magnetic anomalies as isochrons. At the longitude of the Pahemo Fracture Zone, in the central part of the Marie Byrd Land sector, the full-spreading rate during chrons 33–31 (80–68 Myr) was  $60 \text{ mm yr}^{-1}$ , increasing to a maximum of  $74 \text{ mm yr}^{-1}$  at chron 27, and then dropping to  $22 \text{ mm yr}^{-1}$  by chron 22. Spreading rates generally decrease westward. Based upon extrapolation towards the continental margin, we estimate that initial oceanic crust formation in the Bellingshausen sector was at approximately chron 34y (84 Myr) and that it formed rapidly. West of the Proto-Antipodes Fracture Zone, seafloor spreading initiated at chron 33n (79.5 Myr). At rates of  $30\text{--}60 \text{ mm yr}^{-1}$ , the 90 km of inferred extension could be achieved in 1.5 to 3.0 Myr.

[79] We construct an improved set of plate reconstructions utilizing our updated analysis of the Antarctic continental margin to place our local interpretations of Antarctica in context. From these we make inferences regarding the general sequence of events during inception of seafloor spreading, and calculate the subsequent motion history of the Bellingshausen plate, which is the oceanic plate adjacent to the Bellingshausen sector of the continental margin (see auxiliary material). Our preferred interpretation is that the tipline of the spreading ridge and hence initial seafloor formation propagated westward between  $\sim 89$  and 84 Myr. Subsequent motion of the Bellingshausen plate relative to Antarctica was at rates  $<40 \text{ mm yr}^{-1}$  and was most commonly  $5\text{--}20 \text{ mm yr}^{-1}$ . Although we have not attempted a quantitative uncertainty analysis, our predictions that motion direction and rate varied spatially and temporally and involved both

local compression and extension are supported by local geology and geophysics [e.g., *Cunningham et al.*, 2002; *Larter et al.*, 2002; *Gohl*, 2012; *Gohl et al.*, 2011].

[80] Our new data and interpretations are generally consistent with previous analyses that indicate Gondwana breakup along this part of the margin was at  $\sim 84$  Myr, and there was subsequent formation of the Bellingshausen plate east of the Proto-Antipodes Fracture Zone [*Molnar et al.*, 1975; *Stock and Molnar*, 1987; *Cande et al.*, 1995; *Larter et al.*, 2002; *Stock and Cande*, 2002; *Cande and Stock*, 2004; *Eagles et al.*, 2004a, 2004b]. The relatively high rifting rate of  $30\text{--}60\text{ mm yr}^{-1}$  during initial margin formation is consistent with the relatively sharp and symmetrical morphology of the margin, and confirms predictions from numerical models [*van Wijk and Cloetingh*, 2002]. By contrast, subsequent motion of the Bellingshausen plate relative to Antarctica has been slow and complex, and has modified the initial rift morphology to create a broad deformed BPBZ that was strongly affected by migrating patterns of deformation and volcanism.

## Acknowledgments

[81] This project is funded by the Earth System Sciences Research School (ESSReS), an initiative of the Helmholtz Association of German research centers (HGF) at the Alfred Wegener Institute for Polar and Marine Research (AWI). We thank the master, crew and scientists of R/V *Polarstern* and especially the pilots and technicians of HeliService international for their support and assistance. We are grateful to Graeme Eagles for his constructive review, and two other reviewers, who chose to remain anonymous, as well as the numerous people who commented on earlier drafts of the manuscript. Figures 1–7 and 9 as well as Figures A.I–A.VII in Text S1 in the auxiliary material were created using Generic Mapping Tools (GMT) [*Wessel and Smith*, 1991]. We especially thank Paul Wessel for coding extra features into GMT5 overnight.

## References

Andersen, O. B., and P. Knudsen (2009), DNSC08 mean sea surface and mean dynamic topography models, *J. Geophys. Res.*, *114*, C11001, doi:10.1029/2008JC005179.

Blaich, O. A., J. I. Faleide, and F. Tsikalas (2011), Crustal breakup and continent-ocean transition at South Atlantic conjugate margins, *J. Geophys. Res.*, *116*, B01402, doi:10.1029/2010JB007686.

Block, A. E., R. E. Bell, and M. Studinger (2009), Antarctic crustal thickness from satellite gravity: Implications for the Transantarctic and Gamburtsev Subglacial Mountains, *Earth Planet. Sci. Lett.*, *288*(1–2), 194–203, doi:10.1016/j.epsl.2009.09.022.

Boyden, J., R. Müller, M. Gurnis, T. Torsvik, J. Clark, M. Turner, H. Ivey-Law, R. Watson, and J. Cannon (2011), Next-generation plate-tectonic reconstructions using GPlates, in *Geoinformatics: Cyberinfrastructure for the Solid Earth Sciences*, edited by G. Keller and C. Baru, pp. 95–114, Cambridge Univ. Press, Cambridge, U. K.

Cande, S. C., and J. M. Stock (2004), Cenozoic reconstructions of the Australia-New Zealand-South Pacific sector of Antarctica, in *The Cenozoic Southern Ocean: Tectonics, Sedimentation and Climate Change Between Australia and Antarctica*, *Geophys. Monogr. Ser.*, vol. 151, edited by N. F. Exon, J. P. Kennett, and M. J. Malone, pp. 5–18, AGU, Washington, D. C.

Cande, S. C., C. A. Raymond, J. Stock, and W. F. Haxby (1995), Geophysics of the Pitman Fracture Zone and Pacific-Antarctic plate motions during the Cenozoic, *Science*, *270*(5238), 947–953, doi:10.1126/science.270.5238.947.

Cook, R., R. Sutherland, and H. Zhu (1999), *Cretaceous-Cenozoic Geology and Petroleum Systems of the Great South Basin, New Zealand*, *Inst. of Geol. and Nucl. Sci. Monogr.*, vol. 20, 188 pp., Inst. of Geol. and Nucl. Sci., Lower Hutt, New Zealand.

Croon, M. B., S. C. Cande, and J. M. Stock (2008), Revised Pacific-Antarctic plate motions and geophysics of the Menard Fracture Zone, *Geochem. Geophys. Geosyst.*, *9*, Q07001, doi:10.1029/2008GC002019.

Cunningham, A. P., R. D. Larter, P. F. Barker, K. Gohl, and F. O. Nitsche (2002), Tectonic evolution of the Pacific margin of Antarctica: 2. Structure of Late Cretaceous–early Tertiary plate boundaries in the Bellingshausen Sea from seismic reflection and gravity data, *J. Geophys. Res.*, *107*(B12), 2346, doi:10.1029/2002JB001897.

Davy, B. (2006), Bollons Seamount and early New Zealand–Antarctic seafloor spreading, *Geochem. Geophys. Geosyst.*, *7*, Q06021, doi:10.1029/2005GC001191.

Davy, B., K. Hoernle, and R. Werner (2008), Hikurangi Plateau: Crustal structure, rifted formation, and Gondwana subduction history, *Geochem. Geophys. Geosyst.*, *9*, Q07004, doi:10.1029/2007GC001855.

Eagles, G., K. Gohl, and R. Larter (2004a), High-resolution animated tectonic reconstruction of the South Pacific and West Antarctic margin, *Geochem. Geophys. Geosyst.*, *5*, Q07002, doi:10.1029/2003GC000657.

Eagles, G., K. Gohl, and R. D. Larter (2004b), Life of the Bellingshausen plate, *Geophys. Res. Lett.*, *31*, L07603, doi:10.1029/2003GL019127.

Finlay, C. C., et al. (2010), International Geomagnetic Reference Field: The eleventh generation, *Geophys. J. Int.*, *183*(3), 1216–1230, doi:10.1111/j.1365-246X.2010.04804.x.

Gardner, G. H. F., L. W. Gardner, and A. R. Gregory (1974), Formation velocity and density—The diagnostic basics for stratigraphic traps, *Geophysics*, *39*(6), 770–780, doi:10.1190/1.1440465.

Gohl, K. (Ed.) (2007), The expedition ANTARKTIS-XXIII/4 of the Research Vessel *Polarstern* in 2006, *Rep. Polar Mar. Res.*, *557*, Alfred Wegener Inst. for Polar and Mar. Res., Bremerhaven, Germany, doi:10013/epic.27102.d001.

Gohl, K. (Ed.) (2010), The expedition of the Research Vessel *Polarstern* to the Amundsen Sea, Antarctica, in 2010 (ANT-XXVI/3), *Rep. Polar Mar. Res.*, *617*, Alfred Wegener Inst. for Polar and Mar. Res., Bremerhaven, Germany, doi:10013/epic.35668.d001.

Gohl, K. (2012), Basement control on past ice sheet dynamics in the Amundsen Sea Embayment, West Antarctica, *Palaeogeogr. Palaeoclimatol. Palaeoecol.*, doi:10.1016/j.palaeo.2011.02.022, in press.

- Gohl, K., et al. (2007), Geophysical survey reveals tectonic structures in the Amundsen Sea Embayment, West Antarctica [online], in *Antarctica: A Keystone in a Changing World—Online Proceedings of the 10th ISAES*, edited by A. K. Cooper, C. R. Raymond, and the 10th ISAES Editorial Team, *U.S. Geol. Soc. Open File Rep., 2007-1047*, paper 047, doi:10.3133/of2007-1047.srp047.
- Gohl, K., G. Uenzelmann-Neben, E. Weigelt, A. Lindeque, T. Kalberg, G. Kuhn, C. D. Hillenbrand, and R. D. Larter (2011), Sedimentary and glacial processes of the Amundsen Sea Embayment, West Antarctica, paper presented at General Assembly, Eur. Geosci. Union, Vienna, 3–8 April.
- Gradstein, F., J. Ogg, A. Smith, W. Bleeker, and L. Lourens (2004), A new geologic time scale with special reference to Precambrian and Neogene, *Episodes*, 27(2), 83–100.
- Grobys, J. W. G., K. Gohl, and G. Eagles (2008), Quantitative tectonic reconstructions of Zealandia based on crustal thickness estimates, *Geochem. Geophys. Geosyst.*, 9, Q01005, doi:10.1029/2007GC001691.
- Grobys, J., K. Gohl, G. Uenzelmann-Neben, B. Davy, and D. Barker (2009), Extensional and magmatic nature of the Campbell Plateau and Great South Basin from deep crustal studies, *Tectonophysics*, 472(1–4), 213–225, doi:10.1016/j.tecto.2008.05.003.
- Halliday, A. N., D.-C. Lee, S. Tommasini, G. R. Davies, C. R. Paslick, J. G. Fitton, and D. E. James (1995), Incompatible trace elements in OIB and MORB and source enrichment in the sub-oceanic mantle, *Earth Planet. Sci. Lett.*, 133(3–4), 379–395, doi:10.1016/0012-821X(95)00097-V.
- Hellinger, S. J. (1981), The uncertainties of finite rotations in plate tectonics, *J. Geophys. Res.*, 86(B10), 9312–9318, doi:10.1029/JB086iB10p09312.
- Huisman, R., and C. Beaumont (2011), Depth-dependent extension, two-stage breakup and cratonic underplating at rifted margins, *Nature*, 473(7345), 74–78, doi:10.1038/nature09988.
- Kipf, A., R. Werner, K. Gohl, F. Hauff, P. van den Bogaard, and K. Hoernle (2008), Age and origin of magmatism at the Marie Byrd Seamounts (Amundsen Sea), paper presented at General Assembly, Eur. Geosci. Union, Vienna, 13–18 Apr.
- König, M. (2006), Processing of shipborne magnetometer data and revision of the timing and geometry of the Mesozoic break-up of Gondwana, PhD thesis, Univ. of Bremen, Bremen, Germany.
- Larter, R. D., A. P. Cunningham, P. F. Barker, K. Gohl, and F. O. Nitsche (2002), Tectonic evolution of the Pacific margin of Antarctica: 1. Late Cretaceous tectonic reconstructions, *J. Geophys. Res.*, 107(B12), 2345, doi:10.1029/2000JB000052.
- Lindeque, A., and K. Gohl (2010), Western Antarctic palaeostratigraphy: Implications for palaeobathymetry and palaeoclimate modelling, paper presented at IPY Oslo Science Conference, World Meteorol. Organ., Oslo, 8–12 June.
- Llubes, M., N. Florsch, B. Legresy, J.-M. Lemoine, S. Loyer, D. Crossley, and F. Remy (2003), Crustal thickness in Antarctica from CHAMP gravimetry, *Earth Planet. Sci. Lett.*, 212(1–2), 103–117, doi:10.1016/S0012-821X(03)00245-0.
- Luyendyk, B. P. (1995), Hypothesis for Cretaceous rifting of east Gondwana caused by subducted slab capture, *Geology*, 23(4), 373–376, doi:10.1130/0091-7613(1995)023<0373:HFCROE>2.3.CO;2.
- Luyendyk, B. P., D. S. Wilson, and C. S. Siddoway (2003), Eastern margin of the Ross Sea Rift in western Marie Byrd Land, Antarctica: Crustal structure and tectonic development, *Geochem. Geophys. Geosyst.*, 4(10), 1090, doi:10.1029/2002GC000462.
- Mendel, V., M. Munsch, and D. Sauter (2005), MODMAG, a MATLAB program to model marine magnetic anomalies, *Comput. Geosci.*, 31(5), 589–597, doi:10.1016/j.cageo.2004.11.007.
- Molnar, P., T. Atwater, J. Mammerickx, and S. M. Smith (1975), Magnetic anomalies, bathymetry and the tectonic evolution of the South Pacific since the Late Cretaceous, *J. R. Astron. Soc.*, 40(3), 383–420, doi:10.1111/j.1365-246X.1975.tb04139.x.
- National Geophysical Data Center (2007), Marine trackline geophysics data (GEODAS), *Data Announce.*, 2003-MGG-02, NOAA, Boulder, Colo.
- Pilet, S., M. B. Baker, and E. M. Stolper (2008), Metasomatized lithosphere and the origin of alkaline lavas, *Science*, 320(5878), 916–919, doi:10.1126/science.1156563.
- Scheuer, C., K. Gohl, and G. Eagles (2006), Gridded isopach maps from the South Pacific and their use in interpreting the sedimentation history of the West Antarctic continental margin, *Geochem. Geophys. Geosyst.*, 7, Q11015, doi:10.1029/2006GC001315.
- Siddoway, C. S., S. L. Baldwin, P. G. Fitzgerald, C. M. Fanning, and B. P. Luyendyk (2004), Ross Sea mylonites and the timing of intracontinental extension within the West Antarctic rift system, *Geology*, 32(1), 57–60, doi:10.1130/G20005.1.
- Smith, W. H. F., and D. T. Sandwell (1997), Global sea floor topography from satellite altimetry and ship depth soundings, *Science*, 277(5334), 1956–1962, doi:10.1126/science.277.5334.1956.
- Stock, J., and P. Molnar (1987), Revised history of early Tertiary plate motion in the south-west Pacific, *Nature*, 325(6104), 495–499, doi:10.1038/325495a0.
- Stock, J. M., and S. C. Cande (2002), Tectonic history of Antarctic seafloor in the Australia–New Zealand–South Pacific sector: Implications for Antarctic continental tectonics, in *Antarctica at the Close of a Millennium*, edited by J. A. Gamble, D. N. B. Skinner, and S. Henrys, *Bull. R. Soc. N. Z.*, 35, 251–259.
- Storey, B. C., P. T. Leat, S. D. Weaver, R. J. Pankhurst, J. D. Bradshaw, and S. Kelley (1999), Mantle plumes and Antarctica–New Zealand rifting: Evidence from mid-Cretaceous mafic dykes, *J. Geol. Soc. London*, 156(4), 659–671, doi:10.1144/gsjgs.156.4.0659.
- Sutherland, R. (1999), Basement geology and tectonic development of the greater New Zealand region: An interpretation from regional magnetic data, *Tectonophysics*, 308(3), 341–362, doi:10.1016/S0040-1951(99)00108-0.
- Sutherland, R., S. Spasojevic, and M. Gurnis (2010), Mantle upwelling after Gondwana subduction death explains anomalous topography and subsidence histories of eastern New Zealand and West Antarctica, *Geology*, 38(2), 155–158, doi:10.1130/G30613.1.
- van Wijk, J., and S. Cloetingh (2002), Basin migration caused by slow lithospheric extension, *Earth Planet. Sci. Lett.*, 198(3–4), 275–288, doi:10.1016/S0012-821X(02)00560-5.
- Vine, F. J., and D. H. Matthews (1963), Magnetic anomalies over oceanic ridges, *Nature*, 199(4897), 947–949, doi:10.1038/199947a0.
- Watts, A. (1988), Gravity anomalies, crustal structure and flexure of the lithosphere at the Baltimore Canyon Trough, *Earth Planet. Sci. Lett.*, 89(2), 221–238, doi:10.1016/0012-821X(88)90174-4.



- Watts, A. B., and J. D. Fairhead (1999), A process-oriented approach to modeling the gravity signature of continental margins, *Leading Edge*, *18*(2), 258–263, doi:10.1190/1.1438270.
- Wessel, P., and W. H. F. Smith (1991), Free software helps map and display data, *Eos Trans. AGU*, *72*(41), 441, doi:10.1029/90EO00319.
- White, R. S., D. McKenzie, and R. K. O’Nions (1992), Oceanic crustal thickness from seismic measurements and rare Earth element inversions, *J. Geophys. Res.*, *97*(B13), 19,683–19,715, doi:10.1029/92JB01749.
- Winberry, J. P., and S. Anandakrishnan (2004), Crustal structure of the West Antarctic rift system and Marie Byrd Land hotspot, *Geology*, *32*(11), 977–980, doi:10.1130/G20768.1.